A metamagnetic 2D copper(II)-azide complex with 1D ferromagnetism and a hysteretic spin-flop transition†

Gerasimi Lazari,[a] Theocharis C. Stamatatos,[a] Catherine P. Raptopoulou,[b] Vassilis Psycharis,[b] Michael Pissas,[b] Spyros P. Perlepes[a] and Athanassios K. Boudalis*[b]

Received 5th January 2009, Accepted 10th March 2009
First published as an Advance Article on the web 31st March 2009
DOI: 10.1039/b823423j

Compound $[Cu_3(N_3)_6(DMF)_2]_n$ (**1**) was initially obtained in a serendipitous way during efforts to prepare a Cu^{II}/N_3^-/Mebta coordination polymer (Mebta = 1-methylbenzotriazole). With the identity of **1** established by single-crystal crystallography, a rational preparative route to this complex was designed and carried out by reacting $Cu(ClO_4)\cdot 6H_2O$ with two equivalents of NaN_3 in DMF. Complex **1** is a 2D coordination polymer possessing $\mu_{1,1,1}$ and $\mu_{1,1,3}$ azido ligands. Its structure consists of $\{Cu_3(N_3)_6(DMF_2)\}$ repeating units, which form chains that run parallel to the *a* axis; their bridging is achieved through end-on azides. The chains form sheets parallel to the *ab* plane through end-to-end azides. The magnetic properties of **1** have been studied in detail. The complex contains 1D ferromagnetic chains, based on a Cu^{II}_3 repeating unit, which can be viewed as having an $S = 3/2$ ground state. The ferromagnetic chains undergo antiferromagnetic coupling, which is weak enough to be overcome by moderate magnetic fields at 2 K leading to a metamagnetic spin-flop transition at 2.7 T. The transition is first-order, leading to hysteresis of the order of 0.2 T.

Introduction

Azides have served as a valuable tool for magnetochemists in their efforts to construct structures exhibiting interesting and, hopefully, useful magnetic properties.[1] To start with, azides are highly versatile bridging ligands, able to bridge up to 5[2] or 6[3] metal ions (in $\mu_{1,1,1,3,3}$ and $\mu_{1,1,1,3,3,3}$ bridging modes, respectively), while μ_4 azido bridges have in several cases been observed in $\mu_{1,1,1,1}$,[4] $\mu_{1,1,1,3}$[5,6] and $\mu_{1,1,3,3}$[7] bridging modes. In addition to that, and probably more importantly, azides are able to predictably transmit certain types of magnetic exchange, depending on their bridging modes. The general rule is that end-on azides transmit ferromagnetic interactions and that end-to-end azides transmit antiferromagnetic ones. This rule is not without its exceptions, as end-on azides have been shown to transmit antiferromagnetic exchange[8] and end-to-end azides have been shown to transmit ferromagnetic exchange.[9]

The preparation of extended (1D, 2D, 3D) molecular materials exhibiting ferromagnetism or ferromagnetic ordering has been a challenge for magnetochemists, and azides have been a useful tool for obtaining such materials. The usual methods used for the preparation of such materials are either the use of an ancillary ligand within the metal-azide reaction system, or the use of bulky cations that give rise to anionic metal-azide lattices. In an effort to employ the former method for the preparation of extended copper(II)-azide arrays, we tested the use of 1-methylbenzotriazole (Mebta) as an ancillary ligand, in DMF (*N*,*N*′-dimethylformamide). This ligand has provided access to 1D, 2D and 3D coordination polymers with divalent metal ions and dicyanamide or tricyanamide,[10] as well as zero-dimensional transition-metal clusters.[11] Although we could not obtain a "ternary" complex containing Mebta, we were able to isolate a 2D Cu^{II}/N_3^- complex in which the ancillary ligand was the solvent used in the reaction. This contains ferromagnetic chains along one direction, coupled antiferromagnetically to produce a material undergoing a metamagnetic transition. Herein, we report the synthesis, structural and magnetic study of this material.

Results and discussion

Synthesis and IR characterization

We initially came across complex $[Cu_3(N_3)_6(DMF)_2]_n$ (**1**) during our efforts to prepare a Cu^{II}/N_3^-/Mebta coordination polymer. The reaction of $Cu(ClO_4)_2\cdot 6H_2O$, Mebta and NaN_3 in a 1 : 2 : 2 ratio in DMF, using concentrated solutions of the reactants (0.3 M in Cu^{II}) gave dark brown prisms analyzed as $Cu(N_3)_2$(Mebta) (**2**). A limited single-crystal X-ray data set on a poor quality crystal confirmed the empirical formula and revealed a 1D structure consisting of double chains.[12] In an attempt to improve the quality of the structure, we repeated the reaction using the stoichiometric ratio of the reactants (1 : 1 : 2) and a significantly more diluted solution (~0.06 M in Cu^{II}). Upon slow evaporation of the solvent over a long period of time, X-ray quality dark green crystals were isolated. Somewhat to our surprise, the analytical data of a dried sample of the crystals were not consistent with the formulation of **1**. Moreover, the characteristic out-of-plane C–H deformation of coordinated Mebta at ~740 cm^{-1} was not visible in the spectrum. From curiosity we collected a full X-ray data set for a dark green crystal; crystallography revealed that

[a]*Department of Chemistry, University of Patras, 265 04, Patras, Greece*
[b]*Institute of Materials Science, NCSR "Demokritos", 153 10, Aghia Paraskevi Attikis, Greece. E-mail: tbou@ims.demokritos.gr; Fax: +30 210-6503365; Tel: +30 210-6503346*

† CCDC reference number 714455. For crystallographic data in CIF or other electronic format see DOI: 10.1039/b823423j

the Mebta-free compound is the 2D polymer **1**. DMF solutions with intermediate concentrations of the reactants (0.1–0.2 M in Cu^{II}) yield mixtures of **1** and **2** (IR evidence). It seems that there is a competition between DMF and Mebta for Cu^{II} coordination sites. It is likely that the reaction solution contains several species in equilibrium, with factors such as concentrations, relative solubilities, lattice energies, crystallization kinetics and others determining the identity of the isolated products.

With the identity of **1** established, a convenient high-yield synthesis of **1** was easily developed by avoiding the presence of Mebta in the reaction. The straightforward formation of **1** can be represented by eqn (1).

$$3n\mathrm{Cu(ClO_4)_2\cdot 6H_2O} + 6n\mathrm{NaN_3} + 2n\mathrm{DMF} \xrightarrow[\mathrm{Et_2O}]{\mathrm{DMF}} [\mathrm{Cu_3(N_3)_6(DMF)_2}]_n + 6n\mathrm{NaClO_4} \quad (1)$$

Attempts to further increase the yield by adding more Et_2O to the DMF solution led to contamination of **1** with $NaClO_4$ (IR evidence). Thus, the DMF–Et_2O volume ratio (~2 : 1) under the given concentration of the reactants (method B in the Experimental) is the appropriate one for the clean isolation of the product in high yield.

Complexes **1** and **2** seem to be the only isolable product from the $Cu(ClO_4)_2\cdot 6H_2O$–NaN_3–Mebta reaction mixture in DMF. Despite our efforts, we could not obtain anionic or cationic complexes. It should be mentioned that direct reactions of Cu^{II} sources containing anions with a good coordination capacity, namely $Cu(NO_3)_2\cdot 2.5H_2O$ and $CuCl_2\cdot 2H_2O$, with NaN_3 in DMF led also to complex **1**. A final point of synthetic interest is the fact that employment of excess of Mebta in dilute DMF solutions, *e.g.* the 1 : 4 : 2 $Cu(ClO_4)_2\cdot 6H_2O$–Mebta–NaN_3 reaction mixture, does not lead to products containing the Mebta ligand but to **1** instead, indicating that this is the thermodynamically stable complex in reaction systems containing low concentrations of the reactants.

In the IR spectrum, **1** exhibits a strong band at ~2100 cm^{-1} which splits into three components and a medium band at 2044 cm^{-1}; these bands are assigned to the asymmetric stretching mode of the two different types of the azide ligands that are present in the complex.[13] The ν(C=O) and δ(OCN) vibrational modes of the coordinated DMF molecules appear at 1640 and 694 cm^{-1}, respectively.[13] Due to coordination, the ν(C=O) and δ(OCN) bands are shifted to lower and higher wavenumbers, respectively, when compared with the corresponding bands in the spectrum of free DMF.[14]

Description of the structure

Complex **1** crystallizes in the monoclinic $P2_1/n$ space group. Its structure is based on the planar centrosymmetric $\{Cu_3(\mu_{1,1}\text{-}N_3)_4(N_3)_2(DMF)_2\}$ repeating unit. However, for the description of its structure we find it useful to start with the $[Cu_3(\mu_{1,1}\text{-}N_3)_4(N_3)_8(DMF)_2\}^{6-}$ unit (Fig. 1).

Cu(1) is situated on an inversion center, and Cu(2) and Cu(2′) are symmetry related through inversion. For the sake of brevity, from this point on we will refer only to Cu(2) unless otherwise required. The coordination spheres of both Cu(1) and Cu(2) are highly elongated octahedral, as a consequence of the Jahn–Teller effect. For Cu(1), the equatorial bond lengths are 2.009(2) [Cu(1)–N1)] and 1.993(2) Å [Cu(1)–N4)], and the axial ones are 2.579(3) Å [Cu(1)–(N7*), Cu(1)–(N7**)]. For Cu(2), the equatorial bond lengths span the range 1.967(3)–2.020(2) Å, while the axial ones are 2.718(3) [Cu(2)–(N4‴)] and 2.491(3) [Cu(2)–(N9#)] Å.

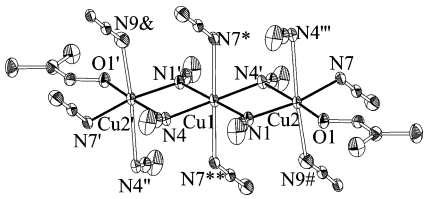

Fig. 1 A partially labelled thermal ellipsoid plot of the basic unit of **1** (′ = –*x*, –*y*, –*z*; ″ = –1 – *x*, –*y*, –*z*; ‴ = 1 + *x*, *y*, *z*; # = 1 – *x*, –1 – *y*, –*z*; * = 1 – *x*, –*y*, –*z*; & = –1 + *x*, 1 + *y*, *z*; ** = –1 + *x*, *y*, *z*).

The bridging between the Cu^{II} atoms within the trinuclear unit is achieved through four azides, which act as $\mu_{1,1}$ bridges if we restrict ourselves within the trinuclear units. The Cu(1)–N–Cu(2) angles are 100.3(1)° for N(1) and 100.0(1)° for N(4′).

These trinuclear repeating units form chains that run parallel to the *a* axis (Fig. 2); their bridging is achieved through end-on azides (donor atoms N(7), N(7*), N(4′), and N(4‴)). Along the *a* axis Cu(1) is bridged to Cu(2*) of an adjacent unit (1 – *x*, –*y*, –*z*) through atom N(7*) of an azide, which acts as a $\mu_{1,1}$ bridge between Cu(1) and Cu(2*), if we restrict ourselves within the 1D chain. Also atoms N(4′) and N(4‴) act as $\mu_{1,1,1}$ bridges, bridging Cu(1) and Cu(2) with Cu(2*), and Cu(2) with Cu(2*) and Cu(1‴). We may thus view the ensemble of Cu(1), Cu(2), Cu(1‴) and Cu(2*) as a defective double cubane.

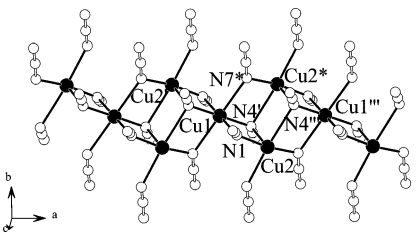

Fig. 2 A portion of the 1D chain formed parallel to the *a* axis, showing the formation of defective double cubanes in **1**. The symmetry operators are the same as in Fig. 1. All DMF molecules have been omitted for clarity.

Finally, these chains form sheets parallel to the *ab* plane (Fig. 3). Inter-chain bridging is achieved by end-to-end azides; Cu(1) is connected to Cu(2%) through N(7*)–N(8*)–N(9*), while Cu(2′) is connected to Cu(1%) and to Cu(2&) through N(7&)–N(8&)–N(9&). The sheets of **1** are isolated from each other by the terminal DMF ligands, which point away from the *ab* plane. The interplane distance is 11.75 Å.

Complex **1** is, to our knowledge, only the third example of a high-dimensionality Cu^{II}/N_3^- complex to contain both $\mu_{1,1,1}$ and $\mu_{1,1,3}$ azide bridges. The first such examples are the structurally related 3D complexes $[Cu_6(N_3)_{12}(N\text{-Eten})_2]_n$ (N-Eten = *N*-ethylethylenediamine) and $\{[Cu_9(N_3)_{18}(1,2\text{-pn})_4]\cdot H_2O\}_n$ (1,2-pn = 1,2-diaminopropane),[5] with both these types of μ_3-azide bridges. Other examples of 2D complexes containing μ_3-azide bridges are the chiral compounds $[Cu(R,R\text{-dacy})(N_3)_2]_n$ and $[Cu(S,S\text{-dacy})(N_3)_2]_n$, (*R*,*R*-dacy and *S*,*S*-dacy are trans-(1*R*,2*R*)- and trans-(1*S*,2*S*)-diaminocyclohexane)[15] and complex $[Cu_2(me2tn)_2(N_3)_4]_n$ (me2tn = 2,2-dimethylpropane-1,3-diamine); these, however, contain only $\mu_{1,1,3}$ bridges.

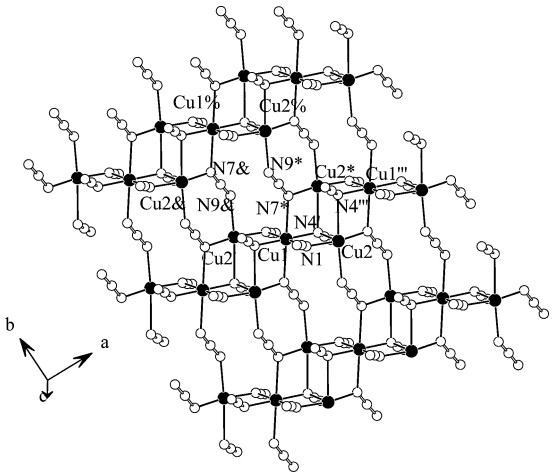

Fig. 3 A sheet formed parallel to the *ab* plane. The symbols of all symmetry operators are the same as in Fig 1, and % = x, 1 + y, z. All DMF molecules have been omitted for clarity.

Magnetic properties

Variable-temperature magnetic susceptibility measurements. $\chi_M T$ and χ_M *vs.* T data for **1** are shown in Fig. 4. The $\chi_M T$ product of **1** at 300 K is 1.28 cm^3 mol^{-1} K, slightly above the value expected for three non-interacting $S = 1/2$ ions (1.24 cm^3 mol^{-1} K for $g = 2.1$). This, along with the increase of $\chi_M T$ upon cooling to a maximum of 2.09 cm^3 mol^{-1} K at 14 K, indicates the interplay of ferromagnetic interactions. Upon further cooling, the $\chi_M T$ product drops abruptly to a value of 0.42 cm^3 mol^{-1} K at 2 K, which is indicative of antiferromagnetic interactions that are operative at low temperatures. On the other hand, the magnetic susceptibility χ_M shows a continuous increase upon cooling, but below 5 K it exhibits a sudden drop, thus revealing a well-defined maximum. This is indicative, as we mentioned, of antiferromagnetic interactions, which are expected to be rather weak, considering the position of the maximum.

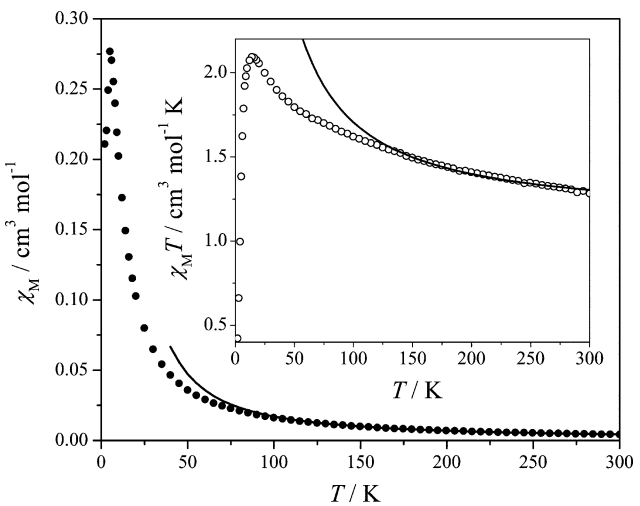

Fig. 4 χ_M *vs.* T and $\chi_M T$ *vs.* T (inset) experimental data for complex **1**, and theoretical curves based on the model described in the text.

Due to the complicated structure of the system, a rigorous interpretation of the magnetic susceptibility data is intractable, since it would require taking into account five different exchange interactions–three intra-chain and two inter-chain ones (see Fig. 5). However, certain simplifications can be considered in order to tackle the problem. It should be made clear though, that we do not assume to undertake an exact treatment of the data; instead, we attempt a semi-quantitative evaluation of the magnetic couplings within **1**. The parameters thus derived will be used to trace the origin of the metamagnetic transition exhibited by **1** (see below).

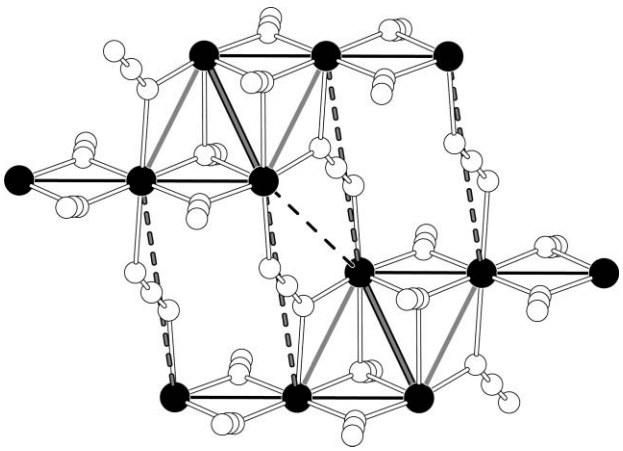

Fig. 5 The full set of magnetic exchange interactions in **1**. Inter-chain interactions are shown as dashed lines.

First of all, we may consider that the exchange coupling will be mainly propagated by bridges directed towards the magnetic orbitals which, for Cu^{II} ions in axially elongated octahedral environments, are of $d_{x^2-y^2}$ character. Thus, the main exchange pathways will be within the 1D chains, since inter-chain bridging is only accomplished through axially coordinated azides. These occupy orbitals of d_{z^2} character, thus the coupling they transmit is expected to be weak, and can be neglected at a first approximation. In any case, however, it is expected to be antiferromagnetic due to the end-to-end inter-chain bridging mode of the azides. Given the lack of superexchange pathways between planes and the large interplane distances (11.75 Å), we can safely assume that the planes are magnetically insulated from each other, with all inter-chain magnetic interactions being constrained within the planes.

When we focus on the 1D chains, we observe that from a magnetic point of view the topology is similar to that of $[Cu_3(CO_3)_2(OH)_2]$ (azurite)[16] and $[Cu_3Cl_6(H_2O)_2(tmso)_2]_n$ (tmso = tetramethylene sulfone),[17] with a topology referred to as "diamond chain". We will refer to the magnetic exchange constant within the trinuclear linear units as J_1, the end-to-middle exchange coupling constants as J_2, and to the end-to-end constants as J_3. The intra-chain spin coupling scheme is shown in Fig. 6.

No exact models are available for the calculation of the magnetic susceptibility of a Heisenberg chain presenting this topology. An exact model for such a topology considers the middle spins as Ising ones to ensure tractability, while assuming $J_1 = J_2$.[18] A model for a Heisenberg chain that explicitly considers three different exchange couplings, uses a 12th order high-temperatures series, and is not accurate at low temperatures.[19] However, this latter model is considered more appropriate, at least for a first understanding of the couplings in **1**.

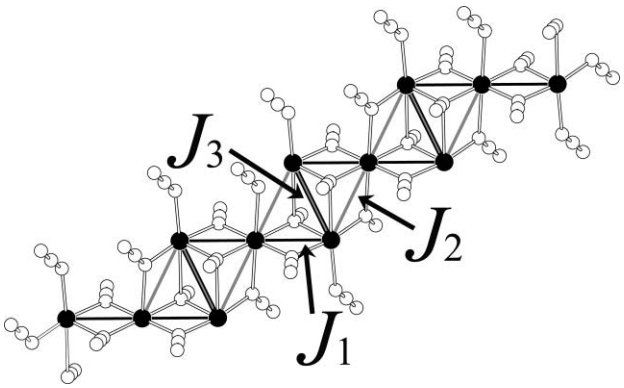

Fig. 6 The intra-chain spin-coupling scheme in **1**, showing the coupling constants used in the fits.

Thus, the magnetic susceptibility was calculated by the relation:

$$\chi_M = \frac{2N_A g^2 \mu_B^2}{k_B}\chi_{red} \quad (2)$$

where χ_{red} is the reduced magnetization expressed as a 12th order series expansion of $1/k_BT$, which takes into account a spin-Hamiltonian formalism of the type JS_iS_j. Due to the length of the exact expression, this is not included herein, but it is supplied in Maple or Mathematica format by the authors.

Various attempts to fit the data revealed that acceptable fits could only be obtained above ~130 K. In all cases, the fitting results showed strong dependence on the temperature range considered and the starting values of the parameters. This was anticipated by the previous use of this model for the interpretation of the magnetic susceptibility data of $[Cu_3Cl_6(H_2O)_2(tmso)_2]_n$, which presented the authors with the same difficulties. Also an underestimation of g was observed like in the above mentioned case; g values of ~2.0 were obtained for most fits, deviating from the typical value of ~2.1 for Cu^{II}.

Thus, a fitting effectuated in the 130–300 K range yielded ferromagnetic couplings with values (using the $-2JS_iS_j$ formalism and expressing coupling constants in cm^{-1})[20] of $J_1 = J_3 = +22\ cm^{-1}$, $J_2 = +6.5\ cm^{-1}$, $g = 2.001$ with $R = 4.2 \times 10^{-5}$. Given the complexity of the system and the limitations of the model, we are not confident of the exact magnitude of the magnetic exchange. However, various fitting attempts showed a clear preference for ferromagnetic couplings, which is in line with the general trend of the magnetic susceptibility data and the structural features of the complex. What was also observed was a tendency of J_1 and J_3 to spontaneously converge to more ferromagnetic values than J_2. We cannot be sure however, whether this bears true physical meaning, or if it is due to an arithmetical convergence of the error-function to specific local minima.

To better understand the system, additional calculations were carried out on a tetrameric $\{Cu_3\}_4$ loop, which was used as an approximation to the 1D chains of **1**. The Cu_{12} system depicted in Fig 6 was topologically transformed into a loop by appropriately connecting the external spins of its edges by the J_1, J_2 and J_3 interactions present in its interior (Scheme 1). Exact calculations were then carried out using the MAGPACK suite,[21] using the ISOMAG and also the ANIMAG version, in order to account for the Zeeman splitting at low temperatures. By using the parameter

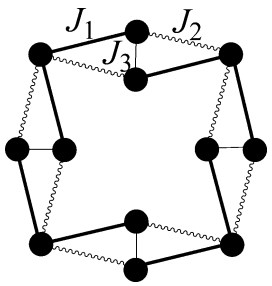

Scheme 1

values defined by the fit, reasonably satisfactory simulations were obtained down to ~100 K, but then diverged to very high $\chi_M T$ values (Fig. 7). It was then considered that the inter-chain interactions should be taken into account. This was accomplished by a mean-field correction considering a zJ interaction between the Cu_{12} loops. This was incorporated into the model through the relation:

$$\chi_{corr} = \frac{\chi_{Cu_{12}}}{1 - \left(\frac{2zJ}{Ng^2\beta^2}\chi_{Cu_{12}}\right)} \quad (3)$$

where $\chi_{Cu_{12}}$ is the susceptibility as calculated by MAGPACK.

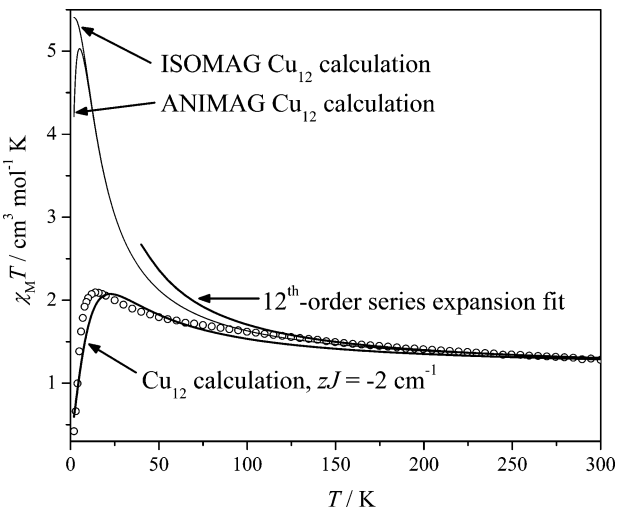

Fig. 7 Experimental and calculated $\chi_M T$ *vs.* T curves for complex **1** according to the models described in the text.

With very small corrections of $zJ = -2\ cm^{-1}$, the calculated curves came to a good qualitative agreement with the experimental ones, while the differences between the anisotropic and isotropic versions became negligible (see Fig. 7). This is in line with our prior assumption that the inter-chain interaction should be weak (due to the participation of non-magnetic orbitals) and antiferromagnetic (due to the end-to-end bridging mode of the azides).

Variable-field magnetization experiments. To complement our studies on this system, we carried out isothermal magnetization experiments at low temperatures, in order to better elucidate its ground-state properties. The data are shown in Fig. 8. At 2 K, the increase of the magnetization M upon increasing field, falls far below the Brillouin values expected for a $S = 3/2$ system. However, this trend is followed by an abrupt increase of the

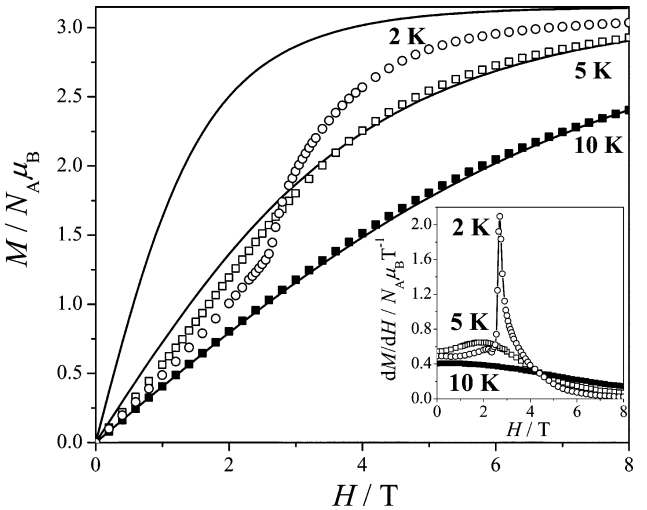

Fig. 8 Magnetization isotherms of **1** at 2 (○), 5 (□) and 10 (■) K, with increasing fields. The lines are Brillouin curves for $S = 3/2$ and $g = 2.1$ at these temperatures. The inset shows the derivatives dM/dH at various temperatures, revealing the 2 K spin-flop field at 2.7 T.

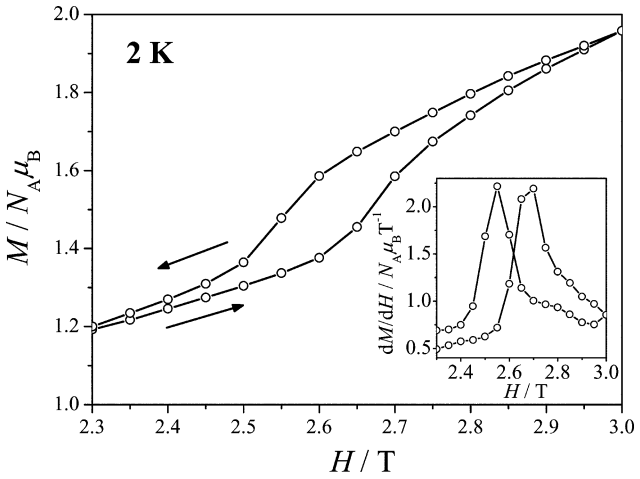

Fig. 9 Hysteresis of the metamagnetic transition at 2 K for complex **1**. The inset shows the derivative dM/dH at the two directions of the field sweep.

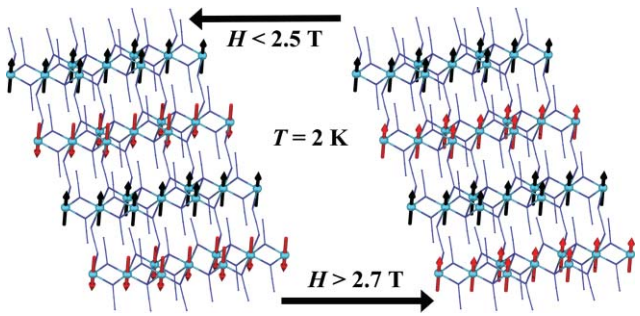

Fig. 10 The proposed mechanism for the metamagnetic spin-flop transition in **1**. The red and black arrows represent the spin alignments within the two antiferromagnetically coupled sublattices. At 2 K, the spin-flop field is different for increasing and decreasing fields.

magnetization above 2.7 T (at 2 K). This increase reveals the onset of a metamagnetic phase transition, while its discontinuity (better illustrated by its derivative) indicates a first-order transition. An onset of saturation above 6 T, at ~$3N_A\mu_B$, is indicative of the trinucler repeating unit of the chains, with an $S = 3/2$ ground state. The isothermal magnetization data at 5 K are smoother, exhibiting a sigmoidal shape and a more gradual transition, arising at ~2 T. At 10 K the antiferromagnetic phase has practically disappeared at zero field. This behaviour reveals that, at low temperatures, the inter-chain antiferromagnetic interactions prevail leading to antiparallel alignment of the magnetic moments of adjacent chains and hence, to antiferromagnetic ordering. This alignment persists until a sufficiently strong field causes the magnetization vectors of the chains to align. A similar case has been previously described for two chiral 2D Cu^{II} materials.[15]

Field-sweep experiments at 2 K, at both increasing and decreasing fields, showed that the spin-flop appears at a lower field value when the magnetic field decreases. This hysteretic behaviour is shown in Fig. 9. Thus, at 2 K, while the spin-flop field is 2.7 T with increasing fields, it appears at 2.5 T with decreasing fields. This suggests the existence of a small magnetic anisotropy for complex **1**.

The proposed mechanism for the metamagnetic behaviour of **1** is depicted in Fig. 10, adopting the concept of the two interpenetrating sublattices, usually employed to describe antiferromagnets. Then, each sublattice would consist of the chains within a plane being next-nearest neighbours to each other.

The hysteretic behaviour observed in **1** has been observed in other metamagnetic materials like $CuCl_2{\cdot}2H_2O$,[22] $FeCl_2$,[23] $CoBr_2{\cdot}6H_2O$,[24] $K_2Fe(Cl_{1-x}Br_x)_5{\cdot}H_2O$ (x = 0.1 and 0.3)[25] and $NiH_2P_2O_7$;[26] however, only $NiH_2P_2O_7$ exhibited a similar magnetic structure giving rise to this effect, *i.e.* ferromagnetic chains with weak antiferromagnetic inter-chain coupling. Although metamagnetic behaviour has been reported in Mn^{II}/N_3^-, Fe^{II}/N_3^- and Ni^{II}/N_3^- coordination polymers,[27] complex **1** is the first example of a Cu^{II}/N_3^- metamagnet.

Conclusions

In our search for high-dimensionality Cu^{II}/N_3^- molecular magnetic materials, we employed an ancillary ligand, namely 1-methylbenzotriazole. Although the reactions carried out with this ligand did not lead to its incorporation into the metal-containing lattice, we managed to obtain an unexpected product, with the reaction solvent itself acting as the ancillary ligand. Complex **1** may prove to be a useful starting material in the area of copper(II)-azide chemistry. From a chemical viewpoint, this result highlights the unpredictability of this type of chemistry, which more often than not, leads to unexpected products.

The complex synthesized was found to form 1D ferromagnetic chains, based on a Cu^{II}_3 repeating unit, which can be viewed as having an $S = 3/2$ ground state. These ferromagnetic chains undergo weak antiferromagnetic coupling, which leads to antiferromagnetic ordering below 5 K. However, this coupling is weak enough to be overcome by moderate fields (2.7 T at 2 K), leading to a metamagnetic spin-flop transition, with a small coercivity (0.2 T). The source of this coercivity is currently unclear. Single-crystal experiments are planned in order to obtain more detailed data and better understand its origin. Efforts are also in progress to improve the quality of the structure of complex $[Cu(N_3)_2(Mebta)]_n$ (**2**) and study its magnetic properties.

Experimental

Materials

All manipulations were carried out under aerobic conditions using all materials and solvents as received. **Caution!** In general, azide and perchlorate salts are potentially explosive and should be handled with care and in small quantities. During the current work in particular, complex **1** was found to explode with friction (scraping from a glass frit with a metallic spatula). For its preparation, only paper filters should be used and only small quantities should be prepared. Use of plastic spatulas is preferable.

Synthesis

Method A. To a stirred solution of Mebta (0.10 g, 0.75 mmol) and NaN_3 (0.10 g, 1.54 mmol) in DMF (12 mL) was added solid $Cu(ClO_4)_2{\cdot}6H_2O$ (0.28 g, 0.76 mmol). The resulting dark brownish green solution was stirred for a further 10 min and left to slowly evaporate at ambient temperature. After 20 d, X-ray quality dark green crystals of **1** were collected by filtration, washed with Et_2O (2×3 mL) and dried *in vacuo*; the yield was 0.10 g (67% based on the metal). $C_6H_{14}N_{20}O_2$ (588.99): calcd C 12.23, H 2.40, N 47.57; found C 12.31, H 2.47, N 46.99. IR data (KBr): 2960 (w), 2938 (w), 2128 (s), 2110 (s) 2080 (s), 2044 (m), 1640 (s), 1490 (w), 1436 (m), 1327 (s), 1296 (w), 1274 (w), 1118 (w), 1060 (w), 694 (m), 652 (w), 584 (w) cm^{-1}.

Method B. To a stirred solution of NaN_3 (0.10 g, 1.54 mmol) in DMF (5 mL) was added solid $Cu(ClO_4)_2{\cdot}6H_2O$ (0.28 g, 0.76 mmol). The solid soon dissolved and the resulting dark green solution layered with Et_2O (3 mL). Slow mixing gave dark green crystals after 2 d. The crystals were collected by filtration, washed with Et_2O (4×2 mL) and dried in air; the yield was 0.12 g (80% based on the metal). The identity of the product was confirmed by elemental analyses and IR spectroscopic comparison with authentic material from method A.

X-Ray crystallography

A dark green crystal of **1** ($0.18 \times 0.20 \times 0.48$ mm) was mounted in air and covered with epoxy glue. Diffraction measurements were made on a Crystal Logic Dual Goniometer diffractometer using graphite monochromated Mo radiation. Important crystal data and parameters for data collection are reported in Table 1. Unit cell dimensions were determined and refined by using the angular settings of 25 automatically centred reflections in the range $11° < 2\theta < 23°$. Three standard reflections monitored every 97 reflections showed less than 3% intensity fluctuation and no decay. Lorentz, polarization corrections were applied using Crystal Logic software. The structure was solved by direct methods using SHELXS-97[28] and refined by full matrix least-squares techniques on F^2 with SHELXL-97.[29] Further experimental crystallographic details for **1**: $2\theta_{max} = 50°$, scan speed 6° min^{-1}; scan range 1.6 + $\alpha_1\alpha_2$ separation; reflections collected/unique/used, 1992/1796[$R_{int} = 0.0163$]/1625; 148 parameters refined; $(\Delta/\sigma)_{max} = 0.003$; $(\Delta\rho)_{max}/(\Delta\rho)_{min} = 0.491/-0.404$ e $Å^{-3}$; $R1$/w$R2$ (for all data), 0.0300/0.0821. Hydrogen atoms were either located by difference maps and were refined isotropically, or were introduced at calculated positions as riding on bonded atoms. All non-H atoms were refined anisotropically.

Table 1 Crystallographic data for complex **1**

	1
Formula	$C_6H_{14}Cu_3N_{20}O_2$
FW	588.95
Space group	$P2_1/n$
T/°C	25
λ/Å	0.71073 (MoKα)
a/Å	5.609(3)
b/Å	7.868(4)
c/Å	23.07(1)
β/°	93.96(1)
V/Å^3	1015.7(9)
Z	2
ρ_{calcd}/g cm^{-3}	1.926
μ(MoKα)/mm^{-1}	3.165
R_1[a]	0.0300[b]
wR_2[a]	0.0793[b]

[a] $w = 1/[\sigma^2(F_o^2) + (aP)^2 + bP]$ and $P = (max)F_o^2,0 + 2F_c^2/3$; $R_1 = \sum(|F_o| - |F_c|)/\sum(|F_o|)$ and $wR_2 = \{\sum[w(F_o^2 - F_c^2)^2]/\sum[w(F_o^2)^2]\}^{1/2}$. [b] For 1625 reflections with $I > 2\sigma(I)$.

Physical measurements

Variable-temperature magnetic susceptibility measurements were carried out on a polycrystalline sample of **1** in the 2–300 K temperature range using a Quantum Design MPMS SQUID susceptometer under a magnetic field of 0.5 T. Diamagnetic corrections for the complex were estimated from Pascal's constants. The magnetic susceptibility has been computed by an analytical expression based on a 12th-order series expansion.[19] Least-squares fittings were accomplished with an adapted version of the function-minimization program MINUIT.[30] The error factor R is defined as $R = \sum \frac{(x_{exp} - x_{calc})^2}{Nx_{exp}^2}$, where N is the number of experimental points. Simulations of the magnetic susceptibility *vs.* temperature in the 2–300 K range were carried out with the MAGPACK program package, using parameters derived from high-temperature fits of the magnetic susceptibility.[21] Magnetization isotherms between 0 and 8 T were collected at 2, 5 and 10 K using a Quantum Design PPMS susceptometer.

References

1 A. Escuer and G. Aromí, *Eur. J. Inorg. Chem.*, 2006, 4721–4736.
2 M. A. S. Goher and F. A. Mautner, *Polyhedron*, 1995, **14**, 1439–1446.
3 G. C. Guo and T. C. W. Mak, *Angew. Chem., Int. Ed.*, 1998, **37**, 3268–3270.
4 See for example: A. K. Boudalis, Y. Sanakis, J. M. Clemente-Juan, B. Donnadieu, V. Nastopoulos, A. Mari, Y. Coppel, J.-P. Tuchagues and S. P. Perlepes, *Chem.–Eur. J.*, 2008, **14**, 2514–2526 and references therein.
5 Z.-G. Gu, J.-L. Zuo and X.-Z. You, *Dalton Trans.*, 2007, 4067–4072.
6 X.-M. Zhang, Y.-F. Zhao, H.-S. Wu, S. R. Batten and S. W. Ng, *Dalton Trans.*, 2006, 3170–3178.
7 (*a*) F. Meyer, P. Kircher and H. Pritzkow, *Chem. Commun.*, 2003, 774; (*b*) S. Demeshko, G. Leibeling, W. Maringgele, F. Meyer, C. Mennerich, H.-H. Klauss and H. Pritzkow, *Inorg. Chem.*, 2005, **44**, 519; (*c*) P. K. Nanda, G. Aromí and D. Ray, *Chem. Commun.*, 2006, 3181; (*d*) G. Fan, S. P. Chen and S. L. Gao, *Struct. Chem.*, 2007, **18**, 725.
8 See for example: S. Saha, S. Koner, J.-P. Tuchagues, A. K. Boudalis, K.-I. Okamoto and D. Mal, *Inorg. Chem.*, 2005, **44**, 6379–6385, and references therein.
9 See references in: T. Liu, Y.-F. Wang, Z.-M. Wang and S. Gao, *Chem.–Asian J.*, 2008, **3**, 950–957.
10 L. F. Jones, L. O'Dea, D. A. Offermann, P. Jensen, B. Moubaraki and K. S. Murray, *Polyhedron*, 2006, **25**, 360–372.

11 K. Skorda, T. C. Stamatatos, A. P. Vafiadis, A. T. Lithoxoidou, A. Terzis, S. P. Perlepes, J. Mrozinski, C. P. Raptopoulou, J. C. Plakatouras and E. G. Bakalbassis, *Inorg. Chim. Acta*, 2005, **358**, 565–582.
12 G. Lazari, C. P. Raptopoulou, V. Psycharis, S. P. Perlepes, A. K. Boudalis, unpublished results.
13 T. C. Stamatatos, G. S. Papaefstathiou, L. R. MacGillivray, A. E. Escuer, R. Vicente, E. Ruiz and S. P. Perlepes, *Inorg. Chem.*, 2007, **46**, 8843.
14 C. Airoldi, *Inorg. Chem.*, 1981, **20**, 998.
15 Y. S. You, J. H. Yoon, H. C. Kim and C. S. Hong, *Chem. Commun.*, 2005, 4116–4118.
16 H. Kikuchi, Y. Fujii, M. Chiba, S. Mitsudo, T. Idehara, T. Tonegawa, K. Okamoto, T. Sakai, T. Kuwai and H. Ohta, *Phys. Rev. Lett.*, 2005, **94**, 227201.
17 (*a*) D. D. Swank and R. D. Willett, *Inorg. Chim. Acta*, 1974, **8**, 143; (*b*) M. Ishii, H. Tanaka, M. Hori, H. Uekusa, Y. Ohashi, K. Tatani, Y. Narumi and K. Kindo, *J. Phys. Soc. Jpn.*, 2000, **69**, 340.
18 L. Čanova, J. Strečka and M. Jaščur, *J. Phys.: Condens. Matter*, 2006, **18**, 4967.
19 A. Honecker and A. Läuchli, *Phys. Rev. B*, 2001, **63**, 174407.
20 The expression proposed by the authors employs the JS_iS_j spin Hamiltonian formalism and expresses coupling constants in K. Under, these conventions, best-fit parameters are: $J_1 = J_3 = -62$ K, $J_2 = -19$ K.
21 (*a*) J. J. Borrás-Almenar, J. M. Clemente-Juan, E. Coronado and B. S. Tsukerblat, *Inorg. Chem.*, 1999, **38**, 6081; (*b*) J. J. Borrás-Almenar, J. M. Clemente-Juan, E. Coronado and B. S. Tsukerblat, *J. Comput. Chem.*, 2001, **22**, 985.
22 M. Date and K. Nagata, *J. Appl. Phys.*, 1963, **34**, 1038–1044.
23 (*a*) I. S. Jacobs and P. E. Lawrence, *Phys. Rev.*, 1967, **164**, 866–878; (*b*) E. Y. Chen, J. F. Drillon and H. J. Guggenheim, *J. Appl. Phys.*, 1977, **48**, 804–807.
24 M. Okaji, J. Kida and T. Watanabe, *J. Phys. Soc. Jpn.*, 1975, **39**, 588–595.
25 A. Paduan-Filho, C. C. Becerra and F. Palacio, *Phys. Rev. B*, 1991, **43**, 11107–11111.
26 T. Yang, J. Ju, G. Li, S. Yang, J. Sun, F. Liao, J. Lin, J. Sasaki and N. Toyota, *Inorg. Chem.*, 2007, **46**, 2342–2344.
27 Y.-F. Zeng, X. Hu, F.-C. Liu, X.-H. Bu, *Chem. Soc. Rev.*, 10.1039/b718581m.
28 G. M. Sheldrick, *SHELXS-97: Structure Solving Program*, University of Göttingen, Germany, 1997.
29 G. M. Sheldrick, *SHELXL97: Crystal Structure Refinement Program*, University of Göttingen, Germany, 1997.
30 F. James and M. Roos, MINUIT Program, a System for Function Minimization and Analysis of the Parameters Errors and Correlations, *Comput. Phys. Commun.*, 1975, **10**, 345.